Jin *et al. Human Genomics* (2025) 19:31
https://doi.org/10.1186/s40246-025-00738-5

Human Genomics

RESEARCH Open Access

# Genetic risk factors associated with ocular perfusion pressure in primary open-angle glaucoma

Heejin Jin[1], Je Hyun Seo[2*], Young Lee[2] and Sungho Won[1,3,4]

## Abstract

**Background** Primary open-angle glaucoma (POAG) is the leading cause of irreversible vision loss. However, its genetic risk factors, such as the vascular hypothesis of POAG, remain unclear. Here, we aimed to explore the genetic associations between mean ocular perfusion pressure (MOPP) and POAG. We performed genome-wide analysis with gene-based analysis from the UK Biobank ($N=459,195$), which includes genetic data and ocular phenotypes. Bidirectional two-sample Mendelian randomisation (MR), multivariable MR, and mediation analysis were conducted using summary statistics from a previous meta-analysis of genome-wide association studies ($N=216,257$).

**Results** *CEP85L*, *GRIA4*, *GRIN2A*, *LRFN5*, *MAGI1*, *POU6F2*, *RBFOX1*, *RBMS1*, *RBMS3*, *RBPMS*, *TRHDE*, *TUBB3*, *ZFHX3*, and *ZMAT4* were significantly correlated with various ocular phenotypes. Furthermore, POAG shared strong genetic associations with corneal resistance factor (CRF), intraocular pressure (IOP), refractive error (RE), and MOPP but none with corneal hysteresis (CH). Univariable MR showed a negative causal effect of CH, CRF, and MOPP and a positive causal effect of IOP on POAG occurrence. In multivariable MR, MOPP exhibited a direct causal effect on POAG, which was supported by the mediation analysis results.

**Conclusions** We successfully determined 14 genetic loci related to CH, CRF, IOP, RE, and MOPP. In univariable and multivaribale MR analyses, a causal effect of MOPP on POAG were observed. In addition, the mediation analysis supported that MOPP exerted direct and indirect causal effects on POAG. This finding indicates that MOPP may serve as a potential causal factor in POAG, providing valuable insights into the pathophysiology of POAG as vascular theory.

**Keywords** Intraocular pressure, Refractive error, Mean ocular perfusion pressure, Glaucoma, Genome-wide association study, Mendelian randomisation, Mediation analysis

*Correspondence:
Je Hyun Seo
jazmin2@naver.com
[1]Institute of Health and Environment, Seoul National University, Seoul, South Korea
[2]Veterans Medical Research Institute, Veterans Health Service Medical Centre, Seoul, South Korea
[3]Department of Public Health Science, Graduate School of Public Health, Seoul National University, Seoul, South Korea
[4]RexSoft Corps, Seoul, South Korea

## Background

Primary open-angle glaucoma (POAG), the leading cause of irreversible vision loss, is a progressive optic neuropathy characterised by degeneration of retinal ganglion cells and their axons; it affects approximately 65 million people worldwide [1, 2]. Alterations in posterior displacement of the lamina cribrosa with blockade of axoplasmic flow are putative features of POAG [3, 4]; however, its precise pathogenesis remains to be elucidated owing to multiple risk factors involved in its pathophysiology [1, 5–7]. The proposed risk factors for POAG include ageing, elevated intraocular pressure (IOP), vascular factors, genetic factors, and ocular phenotypes, such as corneal hysteresis (CH), corneal resistance factor (CRF), and refractive error (RE) [1, 8, 9]. There has been tremendous growth in our understanding of glaucoma genetics over the past decade, with over 125 genes identified as being associated with POAG and more than 100 novel single nucleotide polymorphisms (SNPs) being linked to IOP alone [10]. However, except for IOP, genetic studies on POAG risk factors and their effects are lacking. This is crucial because glaucoma is primarily a complex polygenic disease.

Several studies have suggested that insufficient ocular blood flow is a risk factor for POAG [11–13], consistent with the vascular theory of glaucoma [14–18]. Although autoregulation of blood vessels might compensate for reduced blood flow to a certain extent [19, 20], several studies have shown that a lower mean ocular perfusion pressure (MOPP) may be a risk factor for POAG [6, 21, 22]. Some studies have shown a significant association between MOPP and POAG [18, 23, 24], and fluctuations in MOPP are significantly associated with POAG [23, 24]; however, others have reported a non-significant or limited impact of MOPP on POAG risk [25, 26]. Furthermore, a statistically significant correlation does not indicate a causal relationship, and therefore, a prospective cohort study is necessary to improve our understanding of the effect of MOPP on POAG. Only a few studies have reported a causal association between MOPP and POAG [18, 27]. Investigating MOPP as a risk factor for POAG using genetic data could unveil novel findings for POAG pathology with respect to vascular theory [24].

Mendelian randomisation (MR) is a genetic epidemiological technique that uses genetic variants associated with potential risk factors as instrumental variables (IVs) to assess the causal effects on disease outcomes [28, 29]. In contrast to observational studies, MR analysis uses genetic variants distributed independently in the population and supports causal interference on the effects of risk factors. Previous studies using MR [30–33] have shown that ocular risk factors, such as CH, CRF, IOP, and RE, have a genetic causal association with POAG. To date, no genome-wide association study (GWAS) or MR analysis has been conducted for MOPP. Considering MOPP as a risk factor, it might help unveil currently unknown mechanisms of POAG development. In the present study, we aimed to elucidate representative genetic features of MOPP and investigate whether MOPP is a causal factor for POAG, using MR analysis. Considering the results of a recent study that showed that deep ocular phenotypes such as CH, CRF, IOP, and RE to be associated with the genetic burden in POAG [33], we analysed these phenotypes using mediation and multivariable (MV) MR analysis. We adopted a two-stage approach, which included the following: (1) Discovery of genetic variants related to ocular risk factors of POAG using GWAS. Since large biobanks such as the UK Biobank (UKBB) do not provide summary information on MOPP, we needed to perform GWAS on primary data after obtaining study permission from UKBB (project ID: 96390). (2) Based on the first stage, identification of the causal association of MOPP with POAG using two-sample (TS) MR and MVMR. This study followed the Strengthening and Reporting of Genetic Association Studies (STREGA) guidelines, an extension of the STROBE statement, to ensure robust and transparent reporting of genetic association findings [34].

## Methods

### Study design and sample phenotype

The study protocol was approved by the Institutional Review Board of Veterans Health Service Medical Centre (IRB No. 2022-03-034). The need for informed consent was waived owing to the retrospective nature of the study; the data were anonymised and de-identified. In addition, the UKBB committee approved the project (project ID: 96390) and material transfer agreement. Among the approximately 500,000 samples from UKBB, our analysis included 459,195 individuals of European ancestry, excluding those of other ethnicities. In this study, CH, CRF, IOP, RE, and MOPP were clinically defined as follows: (1) CH (data field id 5256 and 5264) and (2) CRF (data field id 5257 and 5265) were measured using a Reichert Ocular Response Analyzer (Reichert, Inc., Depew, NY) according to a predetermined protocol (available at http://biobank.ctsu.ox.ac.uk/crystal/refer.cgi?id¼100236) provided by UKBB. (3) IOP measurements were based on the corneal compensated IOP (data field id 5254 and 5262) and the maximum value in two eyes. (4) RE (data field id 7390 and 7389) was measured using a Tomey RC 5000 auto-refractor (Tomey GmbH, Germany). The mean spherical equivalent (MSE) was calculated using the following formula: spherical power + (0.5 × cylindrical power). The worse MSE values (across the left and right eyes) were used in our analysis. (5) MOPP was calculated from IOP using the corneal compensated IOP and the maximum value in two eyes

$(\mathrm{MOPP} = \frac{2}{3}\left[\mathrm{DBP} + \frac{1}{3}(\mathrm{SBP} - \mathrm{DBP})\right] - \mathrm{IOP}$, where SBP and DBP denote the systolic and diastolic blood pressure, respectively). UKBB provides two forms of IOP: the Goldmann applanation tonometer-measured IOP (GAT-IOP, data field id 5255 and 5263) and corneal compensated IOP (IOPcc, data field id 5254 and 5262). MOPP can be computed by selecting the average IOP (IOPmean) and highest IOP (IOPmax) of both eyes. Because an individual has two eyes, four types of IOP can be calculated: GAT-IOPmean, GAT-IOPmax, IOPcc_mean, and IOPcc_max; the same applies to MOPP. GWAS analysed four categories of IOP phenotypes, although no significant difference was observed between them owing to their high similarity in the pilot analysis. Because IOPcc is theoretically ideal [35], and IOPmax is better than IOPmean for characterising POAG and the systemic factors that demonstrate the features of IOP, this study defined IOPcc_max as the 'IOP', which was used for calculating the MOPP.

### Genotyping and imputation

Genotyping was performed using the UKBB data, which identified 805,426 single-nucleotide polymorphisms in approximately 500,000 individuals [36]. Sample and SNP quality controls were performed. Samples with sex inconsistencies or call rates of < 95% were excluded from the analysis. SNPs were excluded from the analysis if they had > 5% missingness, a minor allele frequency of < 0.05, or a deviation from the Hardy–Weinberg equilibrium with a $P < 1.00 \times 10^{-6}$. After quality control, imputation was performed with IMPUTE4 using UK10K, 1000 Genomes Phase 3, and the Haplotype Reference Consortium panel as reference data [37]. Therefore, 80,863,435 imputed SNPs were used in the analysis (Fig. 1a).

### Gene-based analysis of GWAS

Genome-wide analysis of CH, CRF, IOP, RE, and MOPP were conducted using a linear model with PLINK [38]. Age, sex, and 10 principal component scores were included as covariates. We performed a gene-based analysis using MAGMA ('generalised gene-set analysis of GWAS data') with our GWAS results as input data [39]. Gene-level analysis was conducted using the SNP-wise mean model (default parameters) to compute *P*-values. European samples from 1000 Genomes Phase 3 were used as a reference panel to adjust for linkage disequilibrium (LD) between SNPs. The input SNPs were mapped to 19,230 protein-coding genes for CH, CRF, and RE and 19,273 protein-coding genes for IOP and MOPP. The significant genes were considered to be those with a false discovery rate (FDR)-adjusted *P*-value ($P_{FDR}$) below 0.05, using the Benjamini–Hochberg procedure [40]. Quantile–quantile (QQ), Manhattan, and colocalisation plots were generated using LocusFocus for the GWAS results [41]. To eliminate the possible confounding effects of population stratification, we calculated the genomic inflation factor (GIF). A GIF value close to 1 indicates the absence of genomic inflation. Furthermore, to investigate

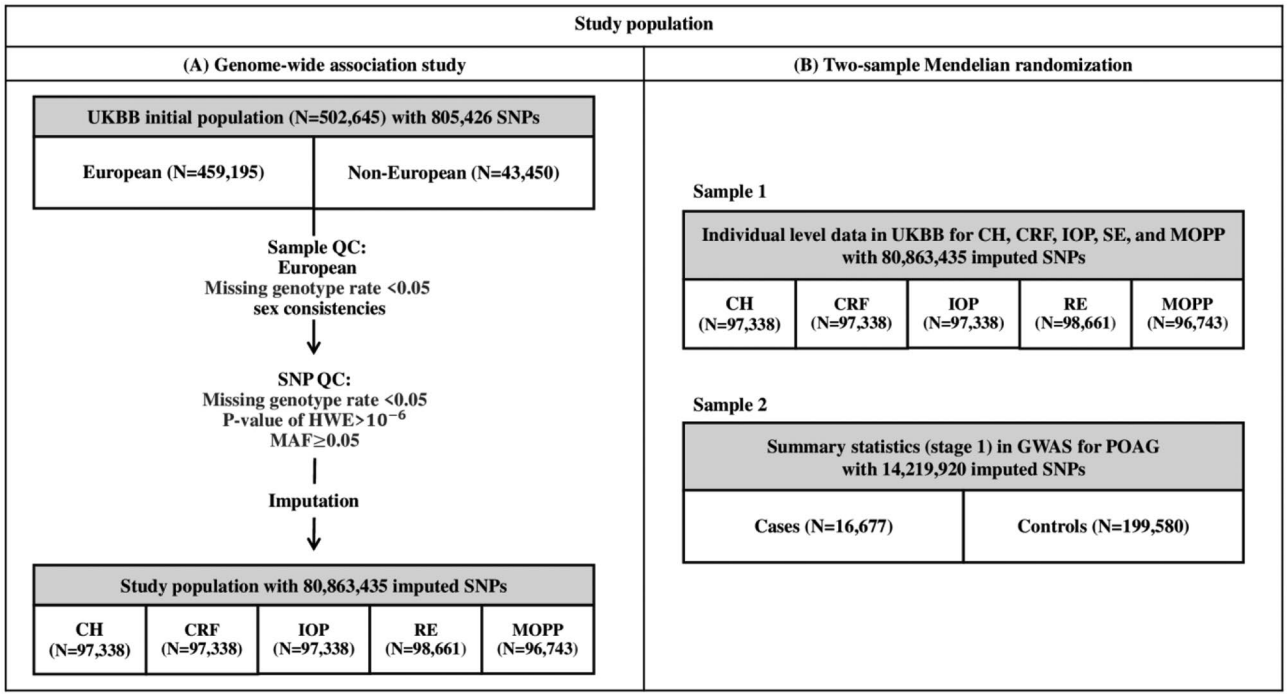


**Fig. 1** Schematic of the selection of the study population. QC, quality control; SNP, single-nucleotide polymorphism; MOPP, mean ocular perfusion pressure; CH, corneal hysteresis; CRF, corneal resistance factor; IOP, intraocular pressure; RE, refractive error; POAG, Primary open-angle glaucoma

the differential expression of significant genes in POAG, we utilised a dataset from the GEO database (accession no.:*GSE27276*) [42]. Differential gene expression analysis was performed using the R package 'limma'.

#### Functional annotation and pathway enrichment analysis

Functional annotation and pathway enrichment analysis were performed using the Database for Annotation, Visualization, and Integrated Discovery (DAVID) tool [43]. The gene list was analysed for associations with diseases (DisGeNET) [44], functional annotations, and gene ontology (GO) terms, as well as enrichment in biological pathways. Specifically, the analysis included the biological process, cellular component, and molecular function categories for GO and pathway databases including KEGG, Reactome, and WikiPathways. An enrichment analysis was conducted using Fisher's exact test, and the results were considered statistically significant when the adjusted *P*-value was less than 0.05.

#### Heritability and genetic correlation (GC)

Heritability of CH, CRF, IOP, RE, and MOPP and their GCs with POAG were estimated using GWAS summary statistics from bivariate LD score regression [45]. The LD reference panel for analysis was based on European ancestry information obtained from the 1000 Genomes Project [46].

#### Instrumental variable selection

The instrumental variables for CH, CRF, IOP, RE, and MOPP were selected from SNPs that showed significant associations in GWAS using the UKBB datasets. The outcome dataset was the summary statistics of a genome-wide meta-analysis of 16,677 cases and 199,580 controls from European samples (Fig. 1b) [47]. To avoid sample overlap, we used GWAS summary statistics from the European samples, excluding the UKBB subjects. To select appropriate IVs for the MR analysis, we utilized the 'ld_clump' function from the R package 'ieugwasr'. This function was applied to perform LD pruning, where variants were excluded based on whether they exhibited strong LD with other variants. Specifically, variants within a 10,000 kb distance or with an LD ($r^2$) greater than 0.001 were removed. Additionally, we excluded variants that were absent from the reference panel to ensure that only high-quality, accessible variants were included. Variants that were nominally associated with POAG ($P < 0.05$) were also removed to minimize any potential bias in the MR analysis. After these quality control steps, we identified the genome-wide SNPs associated with CH, CRF, IOP, RE, and MOPP. Only the SNPs that passed these filtering criteria were selected as IVs for the MR analysis. These steps ensure that the final set of IVs used in the MR analysis are independent, non-pleiotropic, and genetically robust, providing reliable results for assessing causal relationships. *F*-statistics (*F*) indicated instrumental strength, and an *F* value larger than 10 suggested that the analysis was unlikely to be affected by weak instrument bias [48]. To detect pleiotropic outlier SNPs, we used Cochran's Q-test, Rucker's Q' statistic, and MR-PRESSO test [48]. Additionally, the violation extent of the 'NO Measurement Error' (NOME) assumption was quantified using $I^2$ statistics, where $I^2$ values above 90 indicated less estimate dilution in the MR analysis [48].

#### Univariable TSMR bidirectional analysis

Univariable TSMR was used to test the causal inferences between CH, CRF, IOP, RE, MOPP, and POAG. We performed traditional and robust MR analysis using different models. First, we used inverse variance-weighted (IVW) analysis to provide unbiased estimates when all IV assumptions were satisfied [48]. We conducted a leave-one-out sensitivity analysis to evaluate the robustness of our results and to detect any potential influence of individual genetic variants on the overall estimates. By iteratively excluding each SNP, we assessed whether the exclusion of any variant substantially altered the causal estimates, which would indicate any potential heterogeneity or pleiotropy. The MR-Egger method was employed to account for pleiotropic effects and estimate the causal effect [48]. In addition, we applied three extensions to the robust MR methods to relax the assumptions by considering multiple IVs and allowing some to be invalid: (1) robust regression, (2) penalised weights, and (3) penalised robust regression [49]. We conducted reverse MR analysis by switching the roles of the exposure and outcome. MR analysis was performed using the 'TwoSampleMR' and 'MendelianRandomization' packages in R software. The significance threshold for MR was set at 0.01 (0.05/5), considering Bonferroni correction.

In this study, we primarily used the robust and penalized robust MR methods, which focus on selecting the most valid instrumental variables (IVs) and excluding unreliable ones, ensuring more significant and reliable estimates. These methods are particularly effective in minimizing bias from invalid IVs, making them suitable for our analysis.

Additionally, weighted median and mode-based MR methods were also applied as complementary approaches to perform further sensitivity analysis. These methods allow for more flexibility in the inclusion of IVs, offering alternative estimates under different assumptions regarding pleiotropy. While these methods are robust to certain violations, such as the presence of invalid IVs, they may be less powerful in the presence of heterogeneity or pleiotropy, which could lead to non-significant results. In our study, the results from the weighted median and mode-based methods did not reach statistical significance,

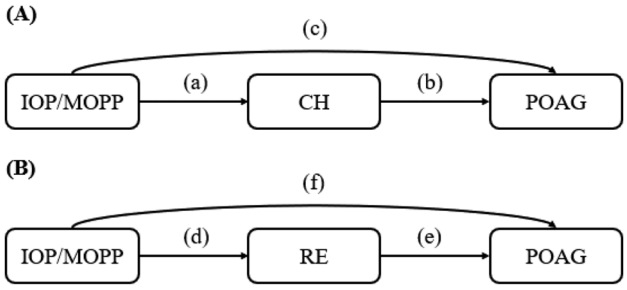


**Fig. 2** Directed acyclic graphs (DAG) for mediation analysis. Path diagram for mediation analysis model with mediators. DAG (**A**) depicts a model where IOP or MOPP are the exposures, CH is the mediator, and POAG is the outcome. DAG (**B**) illustrates a model where IOP or MOPP are the exposures, RE is the mediator, and POAG is the outcome. For the sake of simplicity, the confounders (age and sex) are not shown. The estimates corresponding to (a) through (f) are shown in Table 6. CH, corneal hysteresis; CRF, corneal resistance factor; IOP, intraocular pressure; RE, refractive error, MOPP, mean ocular perfusion pressure; POAG, Primary open-angle glaucoma

possibly due to the inclusion of less robust IVs or the impact of pleiotropy.

#### MV TSMR analysis

MVMR extends univariable (UV) MR by including all phenotypes in the same model and jointly estimating their causal effects on POAG risk. The IVs selected for each phenotype in the UVMR analysis were directly carried over to the MVMR models without modification. Specifically, the same set of SNPs identified as IVs in the UVMR for each individual phenotype was used in the MVMR analysis. Through factor analysis, we selected the variables to include in the MVMR models (Model 1 = CH, IOP, and RE; Model 2 = CH, MOPP, and RE). While UVMR allows us to examine the causal effect of each phenotype individually, MVMR allows for the simultaneous assessment of multiple phenotypes, accounting for potential correlations among the IVs related to each phenotype. This correlation between IVs is explicitly incorporated into the MVMR analysis to ensure the robustness and accuracy of the results. To infer causal effects using MVMR, the analysis was performed using the 'MVMR' package in R software using the MV-IVW and MVMR-Egger methods.

#### Mediation analysis using structural equation models

To estimate the direct and indirect effects using the structural equation modelling (SEM) framework, we assumed a mediation analysis model corresponding to the directed acyclic graph (DAG) in Fig. 2. To reinforce the theoretical foundation of the proposed pathways, additional relevant studies were systematically reviewed and incorporated. Specifically, the study by Wong et al. was included to support the "IOP/MOPP→RE→POAG" pathway [50]. Furthermore, the study by Deol et al. highlighting the physiological interplay in the "IOP/MOPP→CH→POAG" pathway was also reviewed and integrated [51]. These studies were selected based on their relevance to the proposed mechanisms and their contributions to understanding the physiological processes involved in POAG. We evaluated the mediation effects of CH or RE on the causal pathway from IOP/MOPP to POAG using the 'sem' function from the R package 'lavvan.'

**Table 1** Baseline characteristics of UK biobank participants included in the present study

| Characteristics | Mean (SD) or *N* (%) |
|---|---|
| Number of participants | 459,195 |
| Male (%) | 209,929 (45.7%) |
| Age, years | 56.76 (8.02) |
| DBP, mm Hg | 82.16 (10.67) |
| SBP, mm Hg | 139.89 (19.65) |
| IOP, mm Hg | 17.36 (4.80) |
| MOPP, mmHg | 50.19 (8.83) |
| CH, mmHg | 11.41 (2.58) |
| CRF, mmHg | 11.39 (2.76) |
| RE, diopter | -0.64 (2.83) |

SD, standard deviation; DBP, diastolic blood pressure; SBP, systolic blood pressure; IOP, intraocular pressure; MOPP, mean ocular perfusion pressure; *P*, p-value from the chi-square test for categorical variables and t-test for continuous variables; CH, corneal hysteresis; CRF, corneal resistance factor; IOP, intraocular pressure; RE, refractive error, MOPP, mean ocular perfusion pressure

## Results

#### Clinical characteristics of the study population

Sample data from 459,195 European individuals from UKBB, and, of them, 98,661 samples with ocular phenotypes were used for the analysis, and the phenotypic characteristics are summarised in Fig. 1; Table 1. The proportion of male participants was 45.7%, and the mean age of the population was 56.76 years. The mean CH, CRF, IOP, MOPP, and RE were 11.41 mmHg, 11.39 mmHg, 17.36 mmHg, 50.19 mmHg, and −0.64 dioptre, respectively.

#### GWAS analysis

We conducted GWAS using 97,338 samples for CH, CRF, and RE and 96,743 samples for IOP and MOPP with 80,863,435 imputed SNPs. The GIF was 1.107 for CH, 1.018 for CRF, 1.154 for IOP, 1.136 for RE, and 1.162 for MOPP, suggesting no evidence of inflation in the GWAS results. The Manhattan and QQ plots for the gene-based analysis of GWAS allowed visualisation of the distribution of several association signals across the genome and enabled the identification of significant loci associated with the traits of interest [Supplementary Fig. S1 (a)–(e)]. LD clumping was conducted with significant SNPs, whereas SNPs with LD with other variants or those absent from the European LD reference panel were excluded from the results. Among the significant genes

**Table 2** List of significant genes for phenotypes based on differential expression for the retinal ganglion cell

| Phenotype | Gene | Chr | Start | Stop | Nsnps | Nparam | $P_{FDR}$ |
|---|---|---|---|---|---|---|---|
| CH | *MAGI1* | 3 | 65,339,200 | 66,024,509 | 3864 | 429 | $1.14\times10^{-3}$ |
| | *ZFHX3* | 16 | 72,816,784 | 73,093,597 | 1709 | 290 | $4.62\times10^{-2}$ |
| CRF | *RBMS3* | 3 | 29,322,473 | 30,051,886 | 4164 | 372 | $1.55\times10^{-2}$ |
| | *MAGI1* | 3 | 65,339,200 | 66,024,509 | 3864 | 429 | $3.98\times10^{-3}$ |
| | *TRHDE* | 12 | 72,481,046 | 73,059,422 | 2533 | 335 | $4.02\times10^{-2}$ |
| IOP | *POU6F2* | 7 | 39,017,598 | 39,532,694 | 2557 | 7 | $2.08\times10^{-2}$ |
| | *TUBB3* | 16 | 89,987,800 | 90,005,169 | 109 | 16 | $3.18\times10^{-2}$ |
| RE | *RBMS1* | 2 | 161,128,662 | 161,350,305 | 1076 | 140 | $2.36\times10^{-2}$ |
| | *ZMAT4* | 8 | 40,388,109 | 40,755,352 | 2282 | 270 | $2.99\times10^{-5}$ |
| | *GRIA4* | 11 | 105,480,721 | 105,852,819 | 1862 | 186 | $2.62\times10^{-13}$ |
| | *LRFN5* | 14 | 42,076,773 | 42,373,752 | 1636 | 131 | $2.20\times10^{-6}$ |
| | *RBFOX1* | 16 | 6,069,095 | 7,763,340 | 16,640 | 667 | $4.70\times10^{-3}$ |
| | *GRIN2A* | 16 | 9,852,376 | 10,276,611 | 3012 | 228 | $2.18\times10^{-3}$ |
| MOPP | *CEP85L* | 6 | 118,781,935 | 119,031,238 | 1443 | 77 | $1.53\times10^{-3}$ |
| | *RBPMS* | 8 | 30,241,944 | 30,429,778 | 862 | 229 | $8.13\times10^{-5}$ |

CH, corneal hysteresis; CRF, corneal resistance factor; IOP, intraocular pressure; RE, refractive error, MOPP, mean ocular perfusion pressure; Gene, gene symbol; Chr, chromosomal location; Start, chromosomal start location of gene; Stop, chromosomal stop location of gene; Nsnps, number of SNPS annotated to gene; Nparam, number of relevant parameters used in the model; $P_{FDR}$, gene-level P-values corrected by false discovery rate

**Table 3** Differential expression analysis using GEO datasets (*GSE27276*)

| Phenotype | Gene | *GSE27276* (*N* = 36) | | |
|---|---|---|---|---|
| | | B | logFC | *P* |
| CH | *MAGI1* | -2.212 | -0.145 | $4.33\times10^{-3}$ |
| | *ZFHX3* | -3.691 | -0.441 | $2.29\times10^{-2}$ |
| CRF | *RBMS3* | -5.537 | 0.110 | 0.221 |
| | *TRHDE* | -4.596 | -0.076 | $6.64\times10^{-2}$ |
| IOP | *POU6F2* | -6.257 | 0.011 | 0.806 |
| | *TUBB3* | -6.278 | -0.016 | 0.894 |
| RE | *RBMS1* | -5.136 | -0.184 | 0.130 |
| | *ZMAT4* | -3.016 | -0.123 | $1.06\times10^{-2}$ |
| | *GRIA4* | -5.556 | -0.105 | 0.227 |
| | *LRFN5* | -4.005 | -0.132 | $3.29\times10^{-2}$ |
| | *RBFOX1* | -4.016 | 0.178 | $3.33\times10^{-2}$ |
| | *GRIN2A* | -4.024 | 0.097 | $3.36\times10^{-2}$ |
| MOPP | *CEP85L* | NA | NA | NA |
| | *RBPMS* | -2.923 | 1.052 | $9.57\times10^{-3}$ |

B, the B-statistic or log-odds that the gene is differentially expressed; logFC, the Log2-fold change between two experimental conditions; NA, not available; CH, corneal hysteresis; CRF, corneal resistance factor; IOP, intraocular pressure; RE, refractive error, MOPP, mean ocular perfusion pressure

for each phenotype, we identified candidate marker genes based on differential expression for the retinal ganglion cell type [52] (Table 2). We found a total of 14 marker genes [*MAGI1* ($P_{FDR}$ = $1.14\times10^{-3}$) and *ZFHX3* ($P_{FDR}$ = $4.62\times10^{-2}$) for CH; *RBMS3* ($P_{FDR}$ = $1.55\times10^{-2}$), *MAGI1* ($P_{FDR}$ = $3.98\times10^{-3}$), and *TRHDE* ($P_{FDR}$ = $4.02\times10^{-2}$) for CRF; *TUBB3* ($P_{FDR}$ = $3.18\times10^{-2}$) and *POU6F2* ($P_{FDR}$ = $2.08\times10^{-2}$) for IOP; *RBMS1* ($P_{FDR}$ = $2.36\times10^{-2}$), *ZMAT4* ($P_{FDR}$ = $2.99\times10^{-5}$), *GRIA4* ($P_{FDR}$ = $2.62\times10^{-13}$), *LRFN5* ($P_{FDR}$ = $2.20\times10^{-6}$), *RBFOX1* ($P_{FDR}$ = $4.70\times10^{-3}$), and *GRIN2A* ($P_{FDR}$ = $2.18\times10^{-3}$) for RE; *CEP85L* ($P_{FDR}$ = $1.53\times10^{-3}$) and *RBPMS* ($P_{FDR}$ = $8.13\times10^{-5}$) for MOPP]. Of them, *POU6F2* have been reported as a significant marker associated with IOP in the previous study [53]. The co-localisation figures from LocusFocus for each gene are shown in Supplementary Fig. S2 [in the artery (aorta and coronary), heart (left ventricle and atrial appendage) and whole blood tissue]. Furthermore, the decreased expression of *MAGI1* ($P=4.33\times10^{-3}$), *ZFHX3* ($P=2.29\times10^{-2}$), *TRHDE* ($P=6.64\times10^{-2}$), *ZMAT4* ($P=1.06\times10^{-2}$), *LRFN5* ($P=3.29\times10^{-2}$), *RBFOX1* ($P=3.33\times10^{-2}$), *GRIN2A* ($P=3.36\times10^{-2}$), and *RBPMS* ($P=9.57\times10^{-3}$) was associated with POAG in the GEO dataset (*GSE27276*) (Table 3). The functinal annotation and pathway analysis revealed significant enrichment of several biological pathways and molecular functions in neurobiology (Supplementary Table S1).

### Heritability and GC

The estimated heritability for CH, CRF, IOP, RE, and MOPP was 7.4%, 9.5%, 6.9%, 21.0%, and 12.1%, respectively, without inflation in the GWAS results (Table 4). We identified strong shared genetics for CRF, IOP, RE, and MOPP with POAG (GC = – 0.264, $P=4.58\times10^{-7}$ for CRF; GC = – 0.665, $P=8.03\times10^{-25}$ for IOP; GC = 0.130, $P=3.20\times10^{-3}$ for RE; GC = 0.325, $P=3.08\times10^{-16}$ for MOPP). No genetic association was observed between CH and POAG (GC = 0.033, $P=0.552$) (Table 4).

### Univariable TSMR bidirectional analysis

A total of 44, 47, 10, 85, and 8 genome-wide SNPs were associated with CH, CRF, IOP, RE, and MOPP, respectively, and were identified as IVs for MR analysis (Supplementary Table S2). The leave-one-out analysis revealed that no single genetic variant had a disproportionately large effect on the overall estimates, supporting

**Table 4** Heritability and genetic correlation between ocular risk factors and primary open-angle glaucoma estimated by LDSC

| Trait | Heritability | | Genetic correlation with POAG | |
|---|---|---|---|---|
| | $h^2 \pm SE$ | GIF | GC ± SE | *P* |
| CH | 0.074 ± 0.009 | 1.107 | 0.033 ± 0.057 | 0.552 |
| CRF | 0.095 ± 0.010 | 1.018 | -0.264 ± 0.052 | $4.58 \times 10^{-7}$ |
| IOP | 0.069 ± 0.008 | 1.154 | -0.665 ± 0.064 | $8.03 \times 10^{-25}$ |
| RE | 0.210 ± 0.014 | 1.136 | 0.130 ± 0.044 | $3.20 \times 10^{-3}$ |
| MOPP | 0.121 ± 0.009 | 1.162 | 0.325 ± 0.039 | $3.08 \times 10^{-16}$ |

CH, corneal hysteresis; CRF, corneal resistance factor; IOP, intraocular pressure; RE, refractive error, MOPP, mean ocular perfusion pressure; SE, standard error; GIF, genomic inflation factor; GC, genetic correlation; LDSC, linkage disequilibrium score regression; *P*, p-value from LDSC; POAG, primary open-angle glaucoma

the robustness of our findings and the absence of significant heterogeneity or pleiotropy. The results of this analysis are presented in Supplementary Fig. S3. For reverse MR, 11, 17, 5, 9, and 9 genome-wide SNPs associated with POAG were used for CH, CRF, IOP, RE, and MOPP, respectively (Supplementary Table S3). All IVs for bidirectional MR were entirely unrelated to the outcomes ($P > 0.05$). We found no evidence of weak instrument bias ($F > 10$), no violation of the NOME assumption ($I^2 > 90$), and no heterogeneity or outlier pleiotropy (*P* of Q-test, Q'-test, and MR-PRESSO > 0.05) (Supplementary Table S4). The correlation matrix of instruments for all variables (Fig. 3) illustrates the relationships among the genetic instruments, which is essential for evaluating the assumption of instrument independence in the subsequent MVMR analysis. Based on the analysis from the robust and penalised robust MR methods (IVW and MR-Egger), which downweighs outliers, we observed that CH [odds ratio (OR) = 0.998 with $P < 0.001$ for all robust methods], CRF (OR = 0.998 with $P < 0.001$ for all robust methods), and MOPP (OR = 0.998 with $P < 0.001$ for all robust methods) were inversely associated with POAG, whereas IOP (OR = 1.002 with $P = 0.009$ for robust and penalised robust IVW methods) was positively associated with POAG (Fig. 4 and Supplementary Tables S5–S9). However, the association was null when non-robust

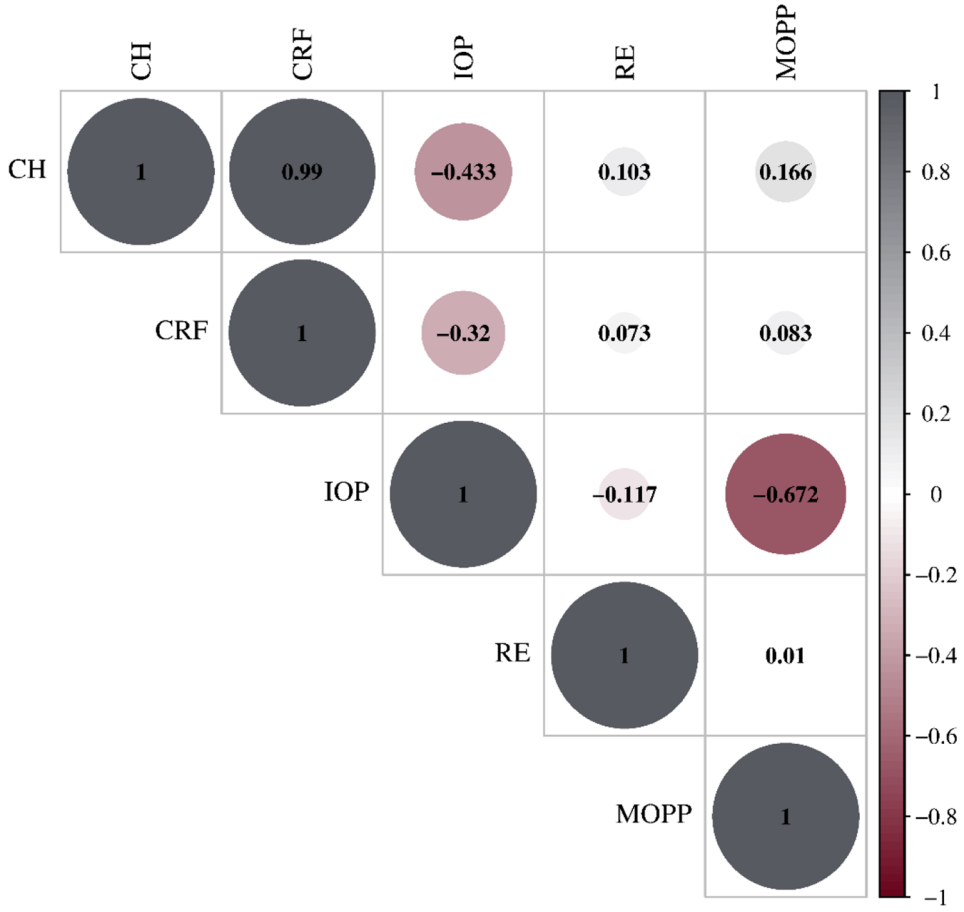


**Fig. 3** Correlation matrix of instruments for all variables in multivariable Mendelian randomization. Grey circles describe variables that have a positive correlation with each other, and red circles describe those that have negative correlations with each other. The size of the circles corresponds to the magnitude of the bivariate correlation. MR, Mendelian randomisation; CH, corneal hysteresis; CRF, corneal resistance factor; IOP, intraocular pressure; RE, refractive error, MOPP, mean ocular perfusion pressure

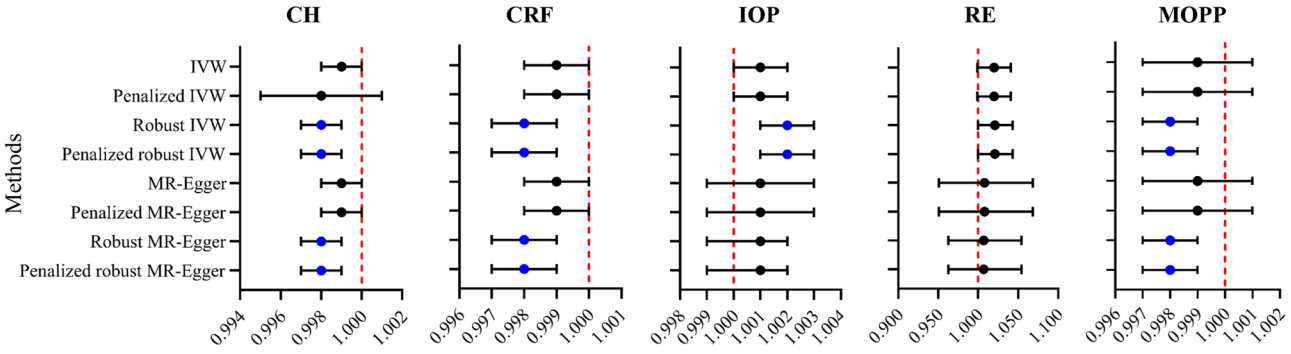


**Fig. 4** Forest plot for univariable MR results. Forest plot showing the univariable MR results for CH, CRF, IOP, RE, and MOPP on POAG risk estimates, which are shown as OR, 95% confidence intervals, and p-values. The X-axis represents the OR, and the red vertical dashed line represents an OR of 1. The Bonferroni correction was used to account for multiple testing. Significant results are highlighted in blue. MR, Mendelian randomisation; IVW, inverse variance weighted; CH, corneal hysteresis; CRF, corneal resistance factor; IOP, intraocular pressure; RE, refractive error, MOPP, mean ocular perfusion pressure; POAG, Primary open-angle glaucoma; OR, odds ratio

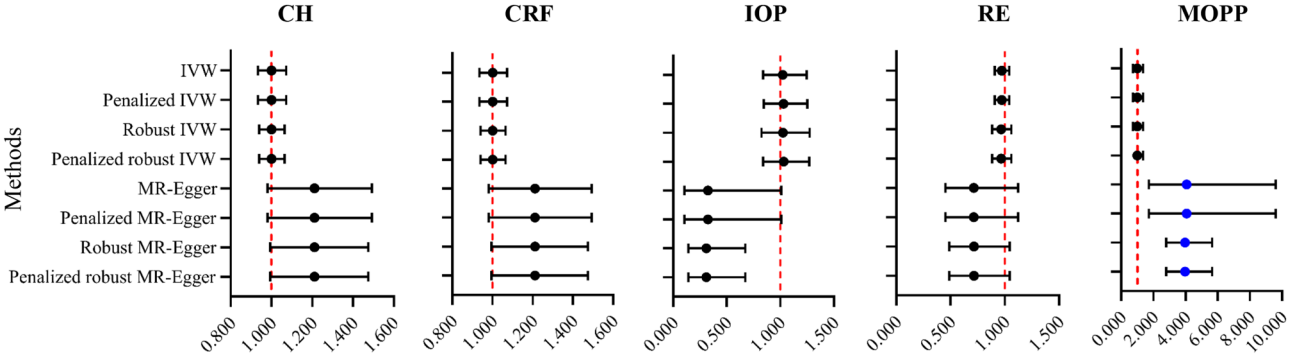


**Fig. 5** Forest plot showing univariable reverse MR results. Forest plot showing the univariable MR results for POAG on CH, CRF, IOP, RE, and MOPP risk estimates, which are shown as OR, 95% confidence intervals, and p-values. The X-axis represents the OR, and the red vertical dashed line represents an OR of 1. The Bonferroni correction was used to account for multiple testing. Significant results are highlighted in blue. MR, Mendelian randomisation; IVW, inverse variance weighted; CH, corneal hysteresis; CRF, corneal resistance factor; IOP, intraocular pressure; RE, refractive error, MOPP, mean ocular perfusion pressure; POAG, Primary open-angle glaucoma; OR, odds ratio

IVW and MR-Egger methods were used. Notably, in the reverse MR-Egger analysis, presence of POAG had significant association with MOPP (OR = 4.066 with $P = 0.001$ for MR-Egger and penalised MR-Egger; OR = 3.971 with $P < 0.001$ for robust MR-Egger and penalised robust MR-Egger) (Fig. 5 and Supplementary Table S9). The intercepts of various MR-Egger methods suggested the presence of horizontal pleiotropy, suggesting that some IVs may influence MOPP through pathways other than POAG. Violation of MR assumption, as is likely in this case, can lead to biased or unreliable estimates. Thus, the findings concerning the impact of POAG on MOPP should be interpreted with caution.

### MV MR analysis

Since the correlation matrix reveals a strong positive correlation between CH and CRF, a negative correlation between CH and IOP, and another negative correlation between IOP and MOPP (Fig. 3). Next, to control for pleiotropic effects, based on the results of factor analysis, we performed an MVMR analysis including CH, IOP, and RE jointly using Model 1, and CH, MOPP and RE jointly using Model 2 (Table 5). In the univariable MR analysis, CH was significant, whereas RE was not; however, in the MVMR analysis, CH ($Ps > 0.05$) was no longer significant and RE (OR = 0.934 with $P < 0.001$ in MV-IVW; OR = 0.929 with $P < 0.001$ in MV-MR-Egger) was significant in Model 1 (Fig. 6 and Supplementary Table S10).

**Table 5** Exploratory factor analysis results

| | Factor 1 | Factor 2 | Factor 3 |
|---|---|---|---|
| CH | 0.98 | 0.13 | 0.02 |
| CRF | 0.98 | 0.09 | 0.00 |
| IOP | -0.03 | -0.85 | -0.03 |
| MOPP | 0.00 | 0.82 | 0.02 |
| RE | 0.01 | 0.03 | 1.00 |
| Proportion of Variance | 0.38 | 0.28 | 0.20 |
| Proportion Explained | 0.38 | 0.66 | 0.86 |
| Cumulative Proportion | 0.44 | 0.77 | 1.00 |

CH, corneal hysteresis; CRF, corneal resistance factor; IOP, intraocular pressure; RE, refractive error, MOPP, mean ocular perfusion pressure

In Model 2, which included MOPP, the intercept of the MVMR-Egger analysis was non-zero, indicating heterogeneity among the IVs. The results in Model 2 revealed that CH (OR = 1.008 with $P = 0.503$) was not significant, whereas RE (OR = 0.945 with $P < 0.001$) was, and MOPP (OR = 0.944 with $P < 0.001$) remained significant (Fig. 6 and Supplementary Table S10).

#### Mediation analysis using structural equation models

Based on the MVMR results assessing the direct effect, it can be inferred that CH, RE, and MOPP has an indirect effect on POAG. The mediation analysis using SEM in the context of a DAG model [Fig. 2, DAG (A)-2 and Table 6] for MOPP, CH, and POAG showed that the mediation effect of MOPP through CH on POAG (a*b) was significant (Estimate = -0.001, $P < 0.001$), indicating a small significant mediation (Table 6). In addition, the mediation analysis [Fig. 2, DAG (B)-2] for MOPP, RE, and POAG demonstrated that both the direct effect of MOPP on POAG (f) and the indirect effect of MOPP through RE on POAG (d*e) were significant (Estimate = -0.002, $P < 0.001$ for both).

## Discussion

In this study, we identified 14 genes related to known risk factors for POAG, including CH, CRF, IOP, RE, and MOPP, through gene-based analysis of GWAS data. After adjusting for all ocular phenotypes using MVMR, we observed a direct effect of RE, IOP, and MOPP on POAG. Importantly, when considering the comprehensive results of UVMR, MVMR, and mediation analysis, it consistently demonstrated that lower MOPP has direct as well as indirect effects on POAG. A previous MR study reported no causal association or a limited effect of blood pressure on POAG [54]. However, our study provides evidence of a consistent and potential association between MOPP and other ocular phenotypes in patients with POAG.

The GWAS results for MOPP and ocular phenotypes are significant, with new features to be declared. Three loci associated with MOPP were also associated with blood pressure [rs7559141 (intergenic *GYPC* and *TEX51*), rs12509595 (intergenic *PRDM8* and *FGF5*), rs2681485 (intronic *ATP2B1*)]. *NPR3* The SNP (rs9292468, intergenic *NPR3* and *LINC02120*) for MOPP

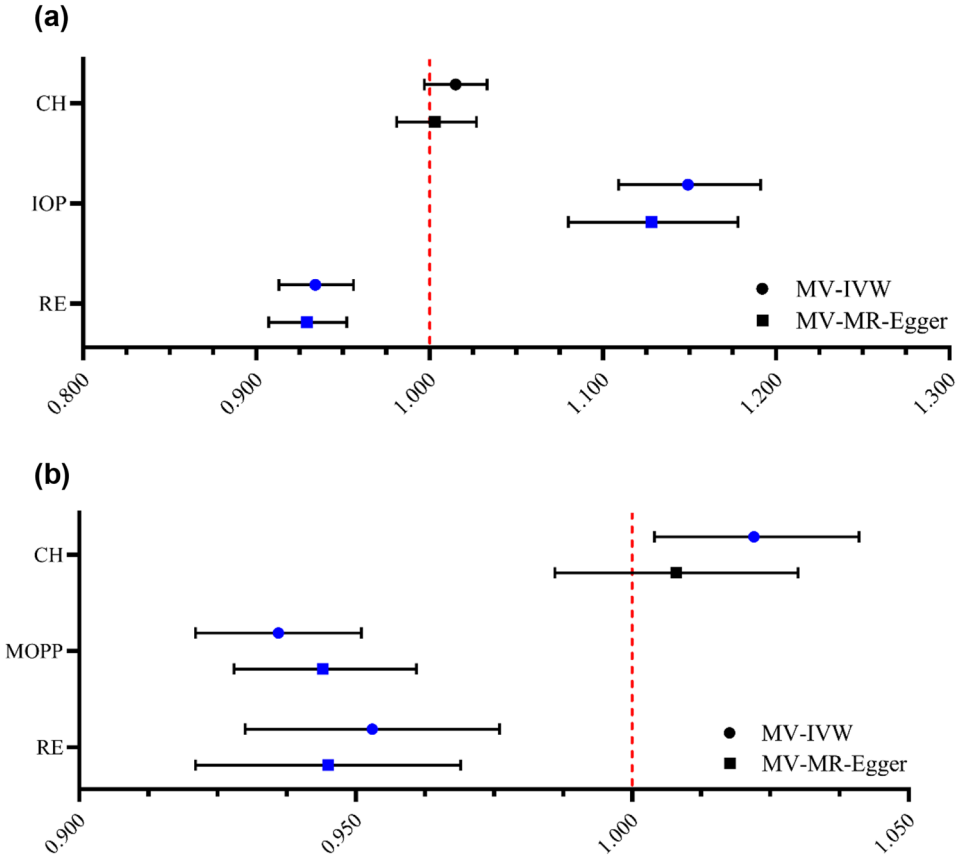


**Fig. 6** Forest plot for multivariable MR results. Forest plot showing the multivariable MR results for model (1) CH, IOP, and RE and model (2) CH, MOPP, and RE on POAG risk estimates, which are shown as odds ratios, 95% confidence intervals, and p-values. Significant results are highlighted in blue. MV, multivariable; MR, Mendelian randomisation; IVW, inverse variance weighted; CH, corneal hysteresis; CRF, corneal resistance factor; IOP, intraocular pressure; RE, refractive error estimated by spherical equivalent; POAG, Primary open-angle glaucoma; MV, multi-variable

**Table 6** Mediation analysis results using SEM

| Path | Estimate | SE | *P* |
|---|---|---|---|
| **DAG (A)-1** | | | |
| IOP → CH (a) | -0.101 | 0.007 | < 0.001 |
| CH → POAG (b) | -0.360 | 0.044 | < 0.001 |
| IOP → POAG (c) | -0.178 | 0.020 | < 0.001 |
| IOP → CH → POAG (a*b) | 0.036 | 0.005 | < 0.001 |
| **DAG (A)-2** | | | |
| MOPP → CH (a) | 0.023 | 0.001 | < 0.001 |
| CH → POAG (b) | -0.002 | 0.000 | < 0.001 |
| MOPP → POAG (c) | -0.002 | 0.000 | < 0.001 |
| MOPP → CH → POAG (a*b) | -0.001 | 0.000 | < 0.001 |
| **DAG (B)-1** | | | |
| IOP → RE (d) | -0.042 | 0.002 | < 0.001 |
| RE → POAG (e) | -0.002 | 0.000 | < 0.001 |
| IOP → POAG (f) | 0.006 | 0.000 | < 0.001 |
| IOP → RE → POAG (d*e) | 0.000 | 0.000 | < 0.001 |
| **DAG (B)-2** | | | |
| MOPP → RE (d) | 0.010 | 0.001 | < 0.001 |
| RE → POAG (e) | -0.003 | 0.000 | < 0.001 |
| MOPP → POAG (f) | -0.002 | 0.000 | < 0.001 |
| MOPP → RE → POAG (d*e) | -0.001 | 0.000 | < 0.001 |

CH, corneal hysteresis; DAG, directed acyclic graphs; IOP, intraocular pressure; RE, refractive error; SE, standard error; MOPP, mean ocular perfusion pressure; POAG, primary open-angle glaucoma; *P*, p-value from SEM; SEM, structural equation models

is related to the natriuretic peptide receptor, which is a secondary signal in the regulation of IOP with a potential link to POAG [55, 56]. In addition, one gene expression study using human tissues from African Americans and Caucasian Americans showed differently expressed *NPR3* in the optic nerve head astrocyte transcriptome [56]. *NPR3* plays an important role in the clearance of natriuretic peptides that modulate blood pressure [57], which might be linked to MOPP and POAG pathogenesis. The SNP, rs4657477 (*TMCO1*) is a well-known POAG locus related to IOP elevation [58–61], and rs28892906 (*AFAP1*) is a well-known locus related to POAG and is independently associated with the IOP and the cup-disc ratio [62, 63], which were found in GWAS. However, these SNPs were not used as IVs due to their potential violation of MR assumptions as confounders.

Enrichment analysis of MOPP-related genes showed that *CEP85L* and *RBPMS* were significantly expressed in retinal ganglion cells in glaucoma. *CEP85L* (centrosomal protein 85 like) is a protein-coding gene related to lissencephaly and plays an essential role in neuronal cell migration. Despite the paucity of glaucoma research on this gene, *CEP85L* has been linked to cardiovascular GWAS for blood pressure [64]. *RBPMS* (RNA binding protein) is a protein-coding gene related to prostate stromal sarcoma and retinal ischaemia via pathway exercise-induced circadian regulation. *RBPMS* is a significant marker for retinal ganglion cells in glaucoma models [65–67]. The discovery of a relationship between these modifications in *RBPMS* and MOPP is notable.

A previous epidemiological study showed that lower systolic, diastolic, and mean perfusion pressures are associated with a higher prevalence of POAG [68], consistent with the results of cross-sectional studies [6, 11, 69]. Forward MR results demonstrated that a lower MOPP can compromise blood flow to the optic nerve head. This ischemic environment may contribute to optic nerve damage, increasing the risk of POAG. This finding aligns with prior evidence that vascular dysregulation and insufficient ocular perfusion play a significant role in glaucoma progression. However, reverse MR results showed that POAG was positively associated with MOPP. Several points should be considered for understanding these results. The significant MR-Egger intercept (Supplementary Tables S9 – S2) highlights the complexity of the relationship between POAG and MOPP, potentially involving shared genetic pathways or confounding factors that cannot be fully accounted for in this analysis. While the MR-Egger slope suggests an inverse association, the limitations of the method and the presence of horizontal pleiotropy call for cautious interpretation of this result. In addition, in this study, the subjects were not strictly controlled in order to study the overall trend of the real-world cohort, MOPP may have increased due to the use of IOP-lowering medication for glaucoma treatment.

It is worthwhile to contrast the findings of this investigation with those of recent studies on the causal relationship between myopia (RE in our study) and POAG [31–33]. A previous study demonstrated that the causal relation between myopia and POAG is mediated by IOP [31], whereas in our study, the causal pathway from MOPP to POAG demonstrated a mediation effect of CH, RE, or both CH and RE. In addition, a study on POAG polygenic risk scores showed that ocular phenotypes, including IOP, CH, and RE, predict the risk stratification of POAG [33], consistent with our findings. The originality of our study lies in the fact that it included MOPP in the model to investigate the role of vascular theory among the risk factors for POAG.

A key strength of our study is its utilisation of a large dataset from UKBB and the analysis of a new clinical dataset, which revealed genetic loci related to ocular phenotypes as risk factors for POAG. Functional annotation and the pathway enrichment analysis revealed the candidate mechanisms related to POAG via identified loci. In addition, through MVMR and mediation analysis, we meticulously analysed the relationships between POAG and ocular phenotypes. However, this study has several limitations. First, our study population is limited to individuals with European ancestry; therefore, concluding the relationship between MOPP and POAG in other ethnic groups is challenging owing to the limited ethnic

diversity of the study population. This limitation can be overcome by conducting replication studies in other ethnic groups, such as East Asian and African populations. Second, it should be understood that the selection of IOP, which prioritized higher values in both eyes, may lead to exaggerated GWAS results. Additionally, the selection of IOP measurement using IOPcc instead of GAT-IOP should also be considered, as it may lead to some differences in clinical settings. Therefore, the findings should be critically evaluated. Third, an aberration in the causal linkage of MOPP to POAG was observed in the reverse MR analysis. However, these results are attributed to the high likelihood of accompanying IOP abnormalities and POAG as opposed to causal effects. Consequently, care must be taken when interpreting the results of reverse MR. Fourth, for the TSMR analysis, we tried to minimise data overlap within UKBB as much as possible. However, approximately 5% of the UKBB dataset does exhibit overlap [47]. Fifith, the discrepancy observed between the UVMR and MVMR analysis, where the protective effect of CF on POAG is seen in UVMR but reversed in MVMR, may be attributed to the differences in the structures of the models. The UVMR analysis evaluates the effect of a single exposure without accounting for potential confounders, whereas MVMR includes multiple exposures and covariates, which could alter the observed relationships. Despite a relatively low correlation between CH and MOPP, which suggests minimal multicollinearity, the inclusion of additional covariates in MVMR may influence the direction of the effect. Further analyses are required to explore the independent effects of CH and MOPP on POAG and to evaluate how confounders interact with these exposures. Finally, if the subjects had any conditions or were using medications that could affect IOP or blood pressure, adjustments might have been necessary; however, no such interventions were made in this study. Since some previous studies applied corrections while others did not [30], we aimed to minimize potentially arbitrary adjustments and analysed the data as they were collected using real-world data for MOPP. Given that the analysis was conducted without applying an operational definition, it can be inferred that, in cases of glaucoma treatment, the use of IOP-lowering drugs effectively led to an increase in MOPP. Hence, further studies with corrections including those for specific ocular conditions may be necessary.

## Conclusions

We successfully determined 14 genetic loci related to CH, CRF, IOP, RE, and MOPP, indicating a potential association with POAG. In addition, a significant genetic causal link was observed between MOPP and POAG. Finally, we found that a lower MOPP has direct and indirect causal effects on POAG. Our findings suggest that, in addition to IOP, MOPP may serve as a potential causal factor of POAG, providing valuable insights into the pathophysiology and vascular theory of POAG.

### Abbreviations

| | |
|---|---|
| CH | Corneal hysteresis |
| CRF | Corneal resistance factor |
| DAG | Directed acyclic graph |
| DAVID | Database for Annotation, Visualization, and Integrated Discovery |
| GC | Genetic correlation |
| GIF | Genomic inflation factor |
| GO | Gene ontology |
| GWAS | Genome-wide association study |
| IOP | Intraocular pressure |
| IVW | Inverse variance-weighted |
| LD | Linkage disequilibrium |
| MOPP | Mean ocular perfusion pressure |
| MR | Mendelian randomisation |
| MSE | Mean spherical equivalent |
| NOME | NO Measurement Error' |
| OR | Odds ratio |
| POAG | Primary open-angle glaucoma |
| RE | Refractive error |
| SEM | Structural equation modelling |
| SNP | Single nucleotide polymorphisms |
| STREGA | Strengthening and Reporting of Genetic Association |

## Supplementary Information

The online version contains supplementary material available at https://doi.org/10.1186/s40246-025-00738-5.

Supplementary Material 1

Supplementary Material 2

### Acknowledgements

This study was conducted using bioresources from UK Biobank (project ID: 96390, Title: Analysis of the association and causality of glaucoma and risk factors (exposure) combined with analysis of genome and image studies; Applicant PI: Jehyun Seo). UK Biobank received ethics approval (11/NW/0382) from the research ethics committee, and participants provided written informed consent.

### Author contributions

HJJ, JHS, YL, and SHW conceived and designed the study and oversaw all analyses; HJJ and SHW performed the GWAS and Mendelian randomisation analysis; HJJ and JHS wrote the primary manuscript; JHS obtained data from the UK Biobank and secured funding; JHS and SHW reviewed the paper and provided key comments. All authors have read and approved the final manuscript.

### Funding

This study was supported by a National Research Foundation of South Korea grant funded by the Government of South Korea (Ministry of Science and ICT No. 2022R1C1C1002929) and by the Veterans Health Service Medical Centre Research Grant (No. VHSMC22045). The funding sources had no role in the design of this study or in the data collection, data analysis, interpretation, writing of the report, or decision to submit results.

### Data availability

The datasets supporting the conclusions of this article are included within the article (its supplementary information as additional file 1: Tables S1–S10 and additional file 2: Figures S1–S3). The GWAS summary statistics data that support the findings of this study (for both multi-ancestry and European-only analyses) are publicly available in the NHGRI-EBI GWAS Catalog at https://www.ebi.ac.uk/gwas/ (access identifier: GCST90011766)UK Biobank data are available at https://www.ukbiobank.ac.uk/enable-your-research/apply-for-access To support the reproducibility of our pipeline, we have made a GitHub

repository to share the scripts for running Mendelian randomisation and follow-up analyses.

## Declarations

**Ethics approval and consent to participate**
The institutional review board of Veterans Health Service Medical Center approved the study protocol (IRB No. 2022-03-034) after the need for informed consent was waived. The UKBB committee approved the project (project ID: 96390) and the material transfer agreements.

**Consent for publication**
Not applicable.

**Competing interests**
The authors declare no competing interests.

Received: 30 September 2024 / Accepted: 2 March 2025
Published online: 24 March 2025

**References**

1. Weinreb RN, Aung T, Medeiros FA. The pathophysiology and treatment of glaucoma: a review. JAMA. 2014;311(18):1901–11.
2. Jayaram H, Kolko M, Friedman DS, Gazzard G. Glaucoma: now and beyond. Lancet. 2023;402(10414):1788–801.
3. Jonas JB, Berenshtein E, Holbach L. Anatomic relationship between lamina Cribrosa, intraocular space, and cerebrospinal fluid space. Invest Ophthalmol Vis Sci. 2003;44(12):5189–95.
4. Strouthidis NG, Fortune B, Yang H, Sigal IA, Burgoyne CF. Effect of acute intraocular pressure elevation on the monkey optic nerve head as detected by spectral domain optical coherence tomography. Invest Ophthalmol Vis Sci. 2011;52(13):9431–7.
5. Jonas JB, Aung T, Bourne RR, Bron AM, Ritch R, Panda-Jonas S. Glaucoma. *Lancet* 2017, 390(10108):2183–2193.
6. Bonomi L, Marchini G, Marraffa M, Bernardi P, Morbio R, Varotto A. Vascular risk factors for primary open angle glaucoma: the Egna-Neumarkt study. Ophthalmology. 2000;107(7):1287–93.
7. Yanagi M, Kawasaki R, Wang JJ, Wong TY, Crowston J, Kiuchi Y. Vascular risk factors in glaucoma: a review. Clin Exp Ophthalmol. 2011;39(3):252–8.
8. Liang L, Zhang R, He LY. Corneal hysteresis and glaucoma. Int Ophthalmol. 2019;39(8):1909–16.
9. Zhang B, Shweikh Y, Khawaja AP, Gallacher J, Bauermeister S, Foster PJ, Eye UK, Vision C. Associations with corneal hysteresis in a population cohort: results from 96 010 UK biobank participants. Ophthalmology. 2019;126(11):1500–10.
10. Khawaja AP, Cooke Bailey JN, Wareham NJ, Scott RA, Simcoe M, Igo RP Jr., Song YE, Wojciechowski R, Cheng CY, Khaw PT, et al. Genome-wide analyses identify 68 new loci associated with intraocular pressure and improve risk prediction for primary open-angle glaucoma. Nat Genet. 2018;50(6):778–82.
11. Tielsch JM, Katz J, Sommer A, Quigley HA, Javitt JC. Hypertension, perfusion pressure, and primary open-angle glaucoma. A population-based assessment. Arch Ophthalmol. 1995;113(2):216–21.
12. Drance SM, Douglas GR, Wijsman K, Schulzer M, Britton RJ. Response of blood flow to warm and cold in normal and low-tension glaucoma patients. Am J Ophthalmol. 1988;105(1):35–9.
13. Flammer J. The vascular concept of glaucoma. Surv Ophthalmol. 1994;38(Suppl):S3–6.
14. Costa VP, Arcieri ES, Harris A. Blood pressure and glaucoma. Br J Ophthalmol. 2009;93(10):1276–82.
15. Seo JH, Kim TW, Weinreb RN, Kim YA, Kim M. Relationship of intraocular pressure and frequency of spontaneous retinal venous pulsation in primary open-angle glaucoma. Ophthalmology. 2012;119(11):2254–60.
16. Schmidl D, Garhofer G, Schmetterer L. The complex interaction between ocular perfusion pressure and ocular blood flow - relevance for glaucoma. Exp Eye Res. 2011;93(2):141–55.
17. Liang Y, Downs JC, Fortune B, Cull G, Cioffi GA, Wang L. Impact of systemic blood pressure on the relationship between intraocular pressure and blood flow in the optic nerve head of nonhuman primates. Invest Ophthalmol Vis Sci. 2009;50(5):2154–60.
18. Costa VP, Harris A, Anderson D, Stodtmeister R, Cremasco F, Kergoat H, Lovasik J, Stalmans I, Zeitz O, Lanzl I, et al. Ocular perfusion pressure in glaucoma. Acta Ophthalmol. 2014;92(4):e252–266.
19. Schmidt KG, Ruckmann AV, Mittag TW, Hessemer V, Pillunat LE. Reduced ocular pulse amplitude in low tension glaucoma is independent of vasospasm. Eye (Lond). 1997;11(Pt 4):485–8.
20. Pillunat LE, Anderson DR, Knighton RW, Joos KM, Feuer WJ. Autoregulation of human optic nerve head circulation in response to increased intraocular pressure. Exp Eye Res. 1997;64(5):737–44.
21. Leske MC, Heijl A, Hyman L, Bengtsson B, Dong L, Yang Z, Group E. Predictors of long-term progression in the early manifest glaucoma trial. Ophthalmology. 2007;114(11):1965–72.
22. Leske MC, Wu SY, Hennis A, Honkanen R, Nemesure B, Group BES. Risk factors for incident open-angle glaucoma: the Barbados eye studies. Ophthalmology. 2008;115(1):85–93.
23. Leske MC. Ocular perfusion pressure and glaucoma: clinical trial and epidemiologic findings. Curr Opin Ophthalmol. 2009;20(2):73–8.
24. Zheng Y, Wong TY, Mitchell P, Friedman DS, He M, Aung T. Distribution of ocular perfusion pressure and its relationship with open-angle glaucoma: the Singapore Malay eye study. Invest Ophthalmol Vis Sci. 2010;51(7):3399–404.
25. Samsudin A, Isaacs N, Tai ML, Ramli N, Mimiwati Z, Choo MM. Ocular perfusion pressure and ophthalmic artery flow in patients with normal tension glaucoma. BMC Ophthalmol. 2016;16:39.
26. Xu L, Wang YX, Jonas JB. Ocular perfusion pressure and glaucoma: the Beijing eye study. Eye (Lond). 2009;23(3):734–6.
27. Raman P, Suliman NB, Zahari M, Kook M, Ramli N. Low nocturnal diastolic ocular perfusion pressure as a risk factor for NTG progression: a 5-year prospective study. Eye (Lond). 2018;32(7):1183–9.
28. Burgess S, Thompson SG. Multivariable Mendelian randomization: the use of pleiotropic genetic variants to estimate causal effects. Am J Epidemiol. 2015;181(4):251–60.
29. Burgess S, Thompson SG. Interpreting findings from Mendelian randomization using the MR-Egger method. Eur J Epidemiol. 2017;32(5):377–89.
30. Simcoe MJ, Khawaja AP, Hysi PG, Hammond CJ, Eye UKB, Vision C. Genome-wide association study of corneal Biomechanical properties identifies over 200 loci providing insight into the genetic etiology of ocular diseases. Hum Mol Genet. 2020;29(18):3154–64.
31. Chong RS, Li H, Cheong AJY, Fan Q, Koh V, Raghavan L, Nongpiur ME, Cheng CY. Mendelian randomization implicates bidirectional association between myopia and primary Open-Angle Glaucoma or intraocular pressure. Ophthalmology. 2023;130(4):394–403.
32. Choquet H, Khawaja AP, Jiang C, Yin J, Melles RB, Glymour MM, Hysi PG, Jorgenson E. Association between myopic refractive error and primary Open-Angle glaucoma: A 2-Sample Mendelian randomization study. JAMA Ophthalmol. 2022;140(9):864–71.
33. Sekimitsu S, Xiang D, Smith SL, Curran K, Elze T, Friedman DS, Foster PJ, Luo Y, Pasquale LR, Peto T, et al. Deep ocular phenotyping across primary Open-Angle Glaucoma genetic burden. JAMA Ophthalmol. 2023;141(9):891–9.
34. Little J, Higgins JP, Ioannidis JP, Moher D, Gagnon F, Von Elm E, Khoury MJ, Cohen B, Davey-Smith G, Grimshaw J. STrengthening the reporting of genetic association studies (STREGA)—an extension of the STROBE statement. Genetic Epidemiology: Official Publication Int Genetic Epidemiol Soc. 2009;33(7):581–98.
35. Morita T, Shoji N, Kamiya K, Hagishima M, Fujimura F, Shimizu K. Intraocular pressure measured by dynamic contour tonometer and ocular response analyzer in normal tension glaucoma. Graefes Arch Clin Exp Ophthalmol. 2010;248(1):73–7.
36. Bycroft C, Freeman C, Petkova D, Band G, Elliott LT, Sharp K, Motyer A, Vukcevic D, Delaneau O, O'Connell J. The UK biobank resource with deep phenotyping and genomic data. Nature. 2018;562(7726):203–9.
37. Howie B, Fuchsberger C, Stephens M, Marchini J, Abecasis GR. Fast and accurate genotype imputation in genome-wide association studies through pre-phasing. Nat Genet. 2012;44(8):955–9.
38. Purcell S, Neale B, Todd-Brown K, Thomas L, Ferreira MA, Bender D, Maller J, Sklar P, De Bakker PI, Daly MJ. PLINK: a tool set for whole-genome association and population-based linkage analyses. Am J Hum Genet. 2007;81(3):559–75.
39. de Leeuw CA, Mooij JM, Heskes T, Posthuma D. MAGMA: generalized gene-set analysis of GWAS data. PLoS Comput Biol. 2015;11(4):e1004219.
40. Love MI, Huber W, Anders S. Moderated Estimation of fold change and dispersion for RNA-seq data with DESeq2. Genome Biol. 2014;15:1–21.

41. Panjwani N, Wang F, Mastromatteo S, Bao A, Wang C, He G, Gong J, Rommens JM, Sun L, Strug LJ. LocusFocus: Web-based colocalization for the annotation and functional follow-up of GWAS. PLoS Comput Biol. 2020;16(10):e1008336.
42. Liu Y, Allingham RR, Qin X, Layfield D, Dellinger AE, Gibson J, Wheeler J, Ashley-Koch AE, Stamer WD, Hauser MA. Gene expression profile in human trabecular meshwork from patients with primary open-angle glaucoma. Investig Ophthalmol Vis Sci. 2013;54(9):6382–9.
43. Huang DW, Sherman BT, Tan Q, Kir J, Liu D, Bryant D, Guo Y, Stephens R, Baseler MW, Lane HC. DAVID bioinformatics resources: expanded annotation database and novel algorithms to better extract biology from large gene lists. Nucleic Acids Res. 2007;35(suppl2):W169–75.
44. Danford ID, Verkuil LD, Choi DJ, Collins DW, Gudiseva HV, Uyhazi KE, Lau MK, Kanu LN, Grant GR, Chavali VRM, et al. Characterizing the POAGome: A bioinformatics-driven approach to primary open-angle glaucoma. Prog Retin Eye Res. 2017;58:89–114.
45. Bulik-Sullivan BK, Loh P-R, Finucane HK, Ripke S, Yang J, Consortium SWGPG, Patterson N, Daly MJ, Price AL, Neale BM. LD score regression distinguishes confounding from polygenicity in genome-wide association studies. Nat Genet. 2015;47(3):291–5.
46. Genomes Project C, Auton A, Brooks LD, Durbin RM, Garrison EP, Kang HM, Korbel JO, Marchini JL, McCarthy S, McVean GA, et al. A global reference for human genetic variation. Nature. 2015;526(7571):68–74.
47. Gharahkhani P, Jorgenson E, Hysi P, Khawaja AP, Pendergrass S, Han X, Ong JS, Hewitt AW, Segre AV, Rouhana JM, et al. Genome-wide meta-analysis identifies 127 open-angle glaucoma loci with consistent effect across ancestries. Nat Commun. 2021;12(1):1258.
48. Jin H, Lee S, Won S. Causal evaluation of laboratory markers in type 2 diabetes on Cancer and vascular diseases using various Mendelian randomization tools. Front Genet. 2020;11:597420.
49. Rees JM, Wood AM, Dudbridge F, Burgess S. Robust methods in Mendelian randomization via penalization of heterogeneous causal estimates. PLoS ONE. 2019;14(9):e0222362.
50. Wong TY, Klein BE, Klein R, Knudtson M, Lee KE. Refractive errors, intraocular pressure, and glaucoma in a white population. Ophthalmology. 2003;110(1):211–7.
51. Deol M, Taylor DA, Radcliffe NM. Corneal hysteresis and its relevance to glaucoma. Curr Opin Ophthalmol. 2015;26(2):96–102.
52. Wang SK, Nair S, Li R, Kraft K, Pampari A, Patel A, Kang JB, Luong C, Kundaje A, Chang HY. Single-cell multiome of the human retina and deep learning nominate causal variants in complex eye diseases. Cell Genomics 2022, 2(8).
53. Gharahkhani P, Jorgenson E, Hysi P, Khawaja AP, Pendergrass S, Han X, Ong JS, Hewitt AW, Segrè AV, Rouhana JM. Genome-wide meta-analysis identifies 127 open-angle glaucoma loci with consistent effect across ancestries. Nat Commun. 2021;12(1):1258.
54. Plotnikov D, Huang Y, Khawaja AP, Foster PJ, Zhu Z, Guggenheim JA, He M. High blood pressure and intraocular pressure: A Mendelian randomization study. Invest Ophthalmol Vis Sci. 2022;63(6):29.
55. Buys ES, Potter LR, Pasquale LR, Ksander BR. Regulation of intraocular pressure by soluble and membrane guanylate cyclases and their role in glaucoma. Front Mol Neurosci. 2014;7:38.
56. Miao H, Chen L, Riordan SM, Li W, Juarez S, Crabb AM, Lukas TJ, Du P, Lin SM, Wise A, et al. Gene expression and functional studies of the optic nerve head astrocyte transcriptome from normal African Americans and Caucasian Americans donors. PLoS ONE. 2008;3(8):e2847.
57. Ren M, Ng FL, Warren HR, Witkowska K, Baron M, Jia Z, Cabrera C, Zhang R, Mifsud B, Munroe PB, et al. The biological impact of blood pressure-associated genetic variants in the natriuretic peptide receptor C gene on human vascular smooth muscle. Hum Mol Genet. 2018;27(1):199–210.
58. Sharma S, Burdon KP, Chidlow G, Klebe S, Crawford A, Dimasi DP, Dave A, Martin S, Javadiyan S, Wood JP, et al. Association of genetic variants in the TMCO1 gene with clinical parameters related to glaucoma and characterization of the protein in the eye. Invest Ophthalmol Vis Sci. 2012;53(8):4917–25.
59. Hysi PG, Cheng CY, Springelkamp H, Macgregor S, Bailey JNC, Wojciechowski R, Vitart V, Nag A, Hewitt AW, Hohn R, et al. Genome-wide analysis of multi-ancestry cohorts identifies new loci influencing intraocular pressure and susceptibility to glaucoma. Nat Genet. 2014;46(10):1126–30.
60. Ozel AB, Moroi SE, Reed DM, Nika M, Schmidt CM, Akbari S, Scott K, Rozsa F, Pawar H, Musch DC, et al. Genome-wide association study and meta-analysis of intraocular pressure. Hum Genet. 2014;133(1):41–57.
61. Burdon KP, Macgregor S, Hewitt AW, Sharma S, Chidlow G, Mills RA, Danoy P, Casson R, Viswanathan AC, Liu JZ, et al. Genome-wide association study identifies susceptibility loci for open angle glaucoma at TMCO1 and CDKN2B-AS1. Nat Genet. 2011;43(6):574–8.
62. Han X, Steven K, Qassim A, Marshall HN, Bean C, Tremeer M, An J, Siggs OM, Gharahkhani P, Craig JE, et al. Automated AI labeling of optic nerve head enables insights into cross-ancestry glaucoma risk and genetic discovery in > 280,000 images from UKB and CLSA. Am J Hum Genet. 2021;108(7):1204–16.
63. Gharahkhani P, Burdon KP, Fogarty R, Sharma S, Hewitt AW, Martin S, Law MH, Cremin K, Bailey JNC, Loomis SJ, et al. Common variants near ABCA1, AFAP1 and GMDS confer risk of primary open-angle glaucoma. Nat Genet. 2014;46(10):1120–5.
64. Litvinukova M, Talavera-Lopez C, Maatz H, Reichart D, Worth CL, Lindberg EL, Kanda M, Polanski K, Heinig M, Lee M, et al. Cells of the adult human heart. Nature. 2020;588(7838):466–72.
65. Kwong JM, Caprioli J, Piri N. RNA binding protein with multiple splicing: a new marker for retinal ganglion cells. Invest Ophthalmol Vis Sci. 2010;51(2):1052–8.
66. Rodriguez AR, de Sevilla Muller LP, Brecha NC. The RNA binding protein RBPMS is a selective marker of ganglion cells in the mammalian retina. J Comp Neurol. 2014;522(6):1411–43.
67. Masin L, Claes M, Bergmans S, Cools L, Andries L, Davis BM, Moons L, De Groef L. A novel retinal ganglion cell quantification tool based on deep learning. Sci Rep. 2021;11(1):702.
68. Memarzadeh F, Ying-Lai M, Chung J, Azen SP, Varma R. Los Angeles Latino eye study G: blood pressure, perfusion pressure, and open-angle glaucoma: the Los Angeles Latino eye study. Invest Ophthalmol Vis Sci. 2010;51(6):2872–7.
69. Quigley HA, West SK, Rodriguez J, Munoz B, Klein R, Snyder R. The prevalence of glaucoma in a population-based study of Hispanic subjects: proyecto VER. Arch Ophthalmol. 2001;119(12):1819–26.


## Publisher's note